The EMBO Journal Vol.16 No.11 pp.3044–3056, 1997

p140mDia, a mammalian homolog of *Drosophila* diaphanous, is a target protein for Rho small GTPase and is a ligand for profilin

Naoki Watanabe[1,2], Pascal Madaule[1], Tim Reid[1,3], Toshimasa Ishizaki[1], Go Watanabe[1], Akira Kakizuka[1], Yuji Saito[1], Kazuwa Nakao[2], Brigitte M.Jockusch[4] and Shuh Narumiya[1,5]

[1]Department of Pharmacology and [2]Department of Medicine and Clinical Science, Kyoto University Faculty of Medicine, Sakyo, Kyoto 606, Japan and [4]Department of Cell Biology, Zoological Institute, Technical University of Braunschweig, D-38106 Braunschweig, Germany

[3]Present address: Faculté de Pharmacie, Université Paris-Sud, INSERM U-461, 5 Rue Jean Baptiste Clement, 92296 Chatenay Malabry Cedex, France

[5]Corresponding author

Rho small GTPase regulates cell morphology, adhesion and cytokinesis through the actin cytoskeleton. We have identified a protein, p140mDia, as a downstream effector of Rho. It is a mammalian homolog of *Drosophila* diaphanous, a protein required for cytokinesis, and belongs to a family of formin-related proteins containing repetitive polyproline stretches. p140mDia binds selectively to the GTP-bound form of Rho and also binds to profilin. p140mDia, profilin and RhoA are co-localized in the spreading lamellae of cultured fibroblasts. They are also co-localized in membrane ruffles of phorbol ester-stimulated sMDCK2 cells, which extend these structures in a Rho-dependent manner. The three proteins are recruited around phagocytic cups induced by fibronectin-coated beads. Their recruitment is not induced after Rho is inactivated by microinjection of botulinum C3 exoenzyme. Overexpression of p140mDia in COS-7 cells induced homogeneous actin filament formation. These results suggest that Rho regulates actin polymerization by targeting profilin via p140mDia beneath the specific plasma membranes.

Keywords: actin polymerization/diaphanous/membrane ruffle/profilin/Rho

Introduction

The actin cytoskeleton plays a central role in cell motility, morphology, phagocytosis and cytokinesis. It is spatially and dynamically reorganized, providing force for the shape change and surface movement in most eukaryotic cells. Rearrangement of actin is evoked rapidly by extracellular stimuli, and sets of actin-associated proteins are thought to act cooperatively in the polymerization, cross-linking and anchorage of actin filaments. The small GTPase Rho has been shown to be required for many actin-dependent cellular processes such as platelet aggregation (Morii *et al.*, 1992), lymphocyte adhesion (Tominaga *et al.*, 1993), cell motility (Takaishi *et al.*, 1993) and cytokinesis (Kishi *et al.*, 1993; Mabuchi *et al.*, 1993). In cultured fibroblasts, microinjection of Rho causes rapid formation of actin stress fibers and focal adhesions. Conversely, inactivation of Rho by botulinum C3 ADP-ribosyltransferase prevents this process (Ridley and Hall, 1992). C3 exoenzyme treatment also blocks lysophosphatidic acid-, endothelin- or GTPγS-induced tyrosine phosphorylation of focal adhesion kinase and paxillin (Kumagai *et al.*, 1993; Rankin *et al.*, 1994; Ridley and Hall, 1994; Seckl *et al.*, 1995). These obsevations indicate that Rho regulates signal transduction pathways linking extracellular stimuli to the reorganization of the actin cytoskeleton.

Recent studies have identified putative downstream target molecules for Rho including citron (Madaule *et al.*, 1995), p150ROK or Rho-kinase or ROCK-II (Leung *et al.*, 1995; Matsui *et al.*, 1996; Nakagawa *et al.*, 1996), p160ROCK (ROCK-I) (Ishizaki *et al.*, 1996), rhophilin and PKN (Watanabe *et al.*, 1996) and rhotekin (Reid *et al.*, 1996). However, the molecular mechanisms by which Rho and these target molecules promote the biological responses described above are poorly understood, although it has been suggested that Rho-kinase down-regulates myosin phosphatase through phosphorylation of a regulatory subunit of this enzyme (Kimura *et al.*, 1996). The involvement of phosphoinositide kinases in Rho signaling has also been reported. Rho (Chong *et al.*, 1994) and Rac (Hartwig *et al.*, 1995), another member of the Rho family of GTPases, were shown in different cell systems to stimulate the synthesis of phosphatidylinositol bisphosphate (PIP_2). Since the binding of PIP_2 is thought to regulate the function of many actin-associated proteins (reviewed by Janmey, 1994; Jockusch *et al.*, 1995), PIP_2 synthesis stimulated by the Rho family of GTPases may induce actin reorganization.

One of the proteins regulated by PIP_2 is profilin, which forms a 1:1 complex with G-actin and which releases actin upon PIP_2 binding. Profilin was thought originally to function in the sequestration of unpolymerized actin in the cytoplasm. Recent studies, however, have demonstrated that profilin itself has a promoting effect on actin polymerization. Profilin stimulates the ADP/ATP exchange of actin (Mockrin and Korn, 1980; Nishida, 1985; Goldschmidt-Clermont *et al.*, 1991) and low amounts of profilin can promote extensive actin assembly in the presence of the thymosin β4–G-actin complex (Pantaloni and Carlier, 1993). The positive effect of profilin on actin polymerization is also supported by *in vivo* data, showing that microinjection of the profilin–actin complex increased the content of filamentous actin beyond the amount of injected actin (Cao *et al.*, 1992). Transient membrane localization of profilin has been noted in activated platelets (Hartwig *et al.*, 1989) and in the membrane ruffles of locomoting cells (Buβ *et al.*,1992; Rothkegel *et al.*, 1996).

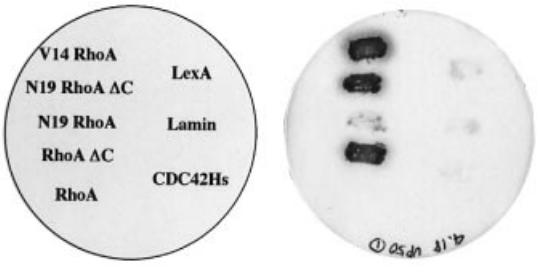

Fig. 1. Interaction of clone 50 peptide with Rho proteins in the two-hybrid system. The L40 yeast strain was co-transformed with pVP-cl.50 obtained from a representative yeast clone, clone 50, and with various LexA–mutant RhoA fusion constructs. The transformants were plated as patches on selective medium, transferred to a cellulose filter and subjected to the β-galactosidase assay (Vojtek *et al.*, 1993). LexA–lamin and LexA alone are used as negative controls. RhoAΔC is a mutant truncated at Ala181. LexA–Val14-RhoAΔC was not used, because it yielded high LacZ activity with the VP-16 activating domain alone.

Focal increases in profilin concentration may, therefore, play an important role in promoting actin polymerization at specific sites in cells, although little is known about the mechanism for recruitment of profilin.

In the present study, we have identified a novel Rho target protein, p140mDia, which is a mammalian homolog of *Drosophila* diaphanous (Castrillon and Wasserman, 1994). p140mDia binds both to the GTP-bound form of RhoA and to profilin through different regions of the molecule. We show that RhoA, p140mDia and profilin are co-localized in the membrane ruffles of rapidly spreading cells and in phagocytic cups induced by fibronectin (FN)-coated beads, both being formed in a Rho-dependent manner.

Results

Isolation of p140mDia partial cDNA in a two-hybrid system

A mouse embryo cDNA library was screened to isolate a novel Rho-binding protein using a yeast two-hybrid system (Vojtek *et al.*, 1993). LexA DNA-binding protein fused to the Asn19-RhoA truncated at Ala181 in the C-terminus (Asn19–RhoAΔC) was used as bait. Among the His(+) and LacZ(+) yeast clones, 55 were selected which showed no LacZ activity with lamin used as a negative control. The clones yielded cDNA inserts of the same size, several of which were sequenced and found to be identical. When these clones were mated to AMR70 strains bearing a LexA fused to various RhoA mutants, they showed an interaction that was strongest with Val14-RhoA, weak with Asn19-RhoA and almost negligible with wild-type RhoA, although they retained strong interaction with Asn19–RhoAΔC or wild-type RhoAΔC. This specificity was confirmed by co-transforming the L40 strain with a plasmid recovered from a representative clone, clone 50, and with various LexA–mutant RhoA fusion constructs (Figure 1). These results suggest that a peptide encoded by clone 50 cDNA preferentially interacts with the activated form of RhoA.

Specific association of p140mDia with the GTP-bound form of RhoA in vitro

The polypeptide encoded by the cDNA isolated above was expressed in *Escherichia coli* either as a His-tagged protein (His_6-cl.50) or as a GST fusion protein (GST–cl.50). An antiserum specific to p140mDia was raised against His_6-cl.50. The specificity of the antiserum was verified by its reactivity with GST–cl.50 expressed in *E.coli* after isopropyl-β-D-thiogalactopyranoside (IPTG) induction (Figure 2A, lanes 1 and 2). The antiserum detected a single band in Swiss 3T3 cell lysates, which migrated to the 160 kDa position on SDS–PAGE (lanes 3 and 4). We designated this protein as p140mDia (see below). Using this antiserum, we examined the binding specificity of p140mDia for the GTP- or GDP-bound form of Rho family GTPases. p140mDia was precipitated from Swiss 3T3 lysates only by the GTPγS-bound form of GST–RhoA but not by the GDP-bound form, GST–Rac1 or GST–Cdc42Hs (Figure 2B). These observations confirm

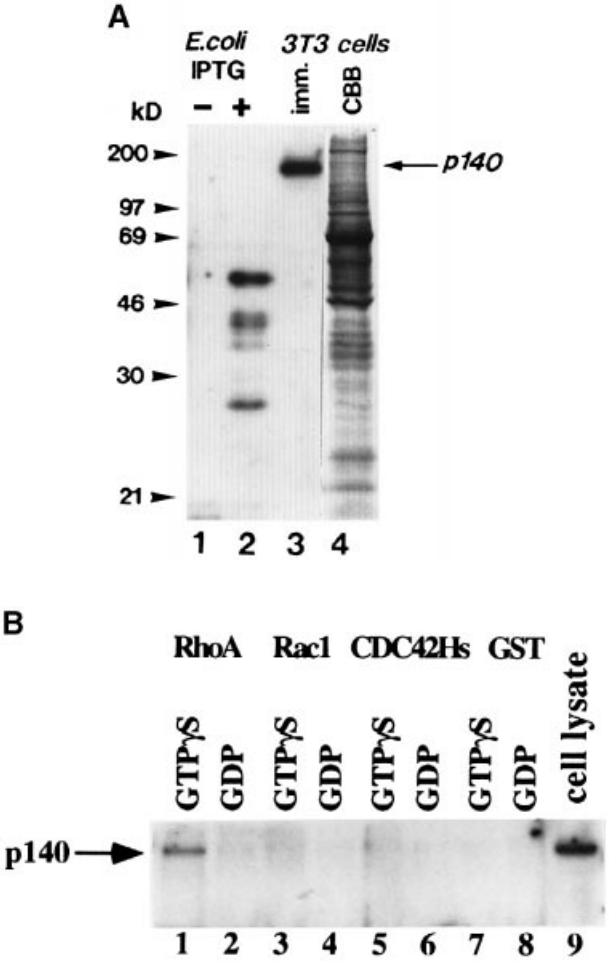

Fig. 2. Specific association of p140mDia with the GTP-bound form of RhoA *in vitro*. (**A**) Specificity of anti-p140 antibody. An antiserum was raised against a His_6-tagged clone 50 polypeptide, and its specificity was examined by Western blotting against total lysates of *E.coli* expressing the GST fusion protein of clone 50 polypeptide before (lane 1) and after IPTG induction (lane 2) or against total lysates of cultured Swiss 3T3 cells (lane 3). Lane 4 shows protein staining with Coomassie brilliant blue of the same sample shown in lane 3. The antiserum was used at a 1:1000 dilution. (**B**) Precipitation of p140mDia by the GTPγS-bound form of RhoA. Swiss 3T3 cell lysates were incubated with GST–RhoA, GST–Rac1, GST–Cdc42Hs or GST, which were pre-loaded with either GTPγS or GDP. GST fusion proteins were precipitated by glutathione–Sepharose 4B and the pellets were analyzed by immmunoblotting with the anti-p140mDia antiserum. Lane 9 shows p140mDia present in one-tenth of the cell lysates used in precipitation.

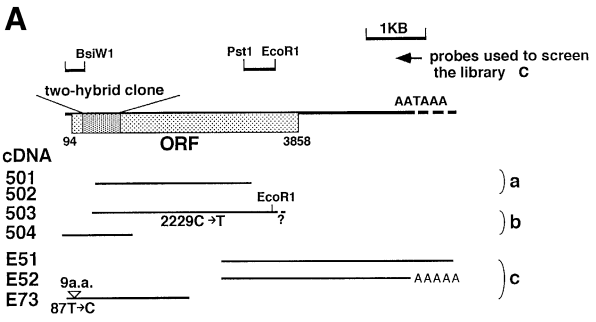

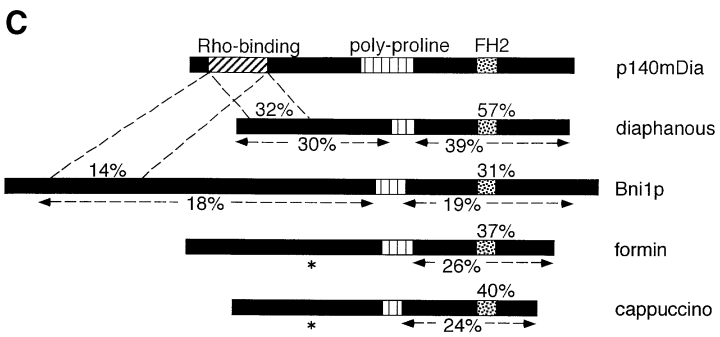

B

```
MEPSGGGLGP GRGTRDKKKG RSPDELPATG GDGGKHKKFL ERFTSMRIKK   50
EKEKPNSAHR NSSASYGDDP TAQSLQDISD EQVLVLFEQM LVDMNLNEEK  100
QQPLREKDIV IKREMVSQYL HTSKAGMNQK ESSRSAMMYI QELRSGLRDM  150
HLLSCLESLR VSLNNNPVSW VQTFGAEGLA SLLDILKRLH DEKEETSGNY  200
DSRNQHEIIR CLKAFMNNKF GIKTMLETEE GILLLVRAMD PAVPNMMIDA  250
AKLLSALCIL PQPEDMNERV LEAMTERAEM DEVERFQPLL DGLKSGTSIA  300
LKVGCLQLIN ALITPAEELD FRVHIRSELM RLGLHQVLQE LREIENEDMK  350
VQLCVFDEQG DEDFFDLKGR LDDIRMEMDD FGEVFQIILN TVKDSKAEPH  400
FLSILQHLLL VRNDYEARPQ YYKLIEECVS QIVLHKNGTD PDFKCRHLQI  450
DIERLVDQMI DKTKVEKSEA KATELEKKLD SELTARHELQ VEMKKMENDF  500
EQKLQDLQGE KDALDSEKQQ ITAQKQDLEA EVSKLTGEVA KLSKELEDAK  550
NEMASLSAVV VAPSVSSSAA VPPAPPLPGD SGTVIPPPPP PPPLPGGVVP  600
PSPPLPPGTC IPPPPPLPGG ACIPPPPQLP GSAAIPPPPP LPGVASIPPP  650
PPLPGATAIP PPPPLPGATA IPPPPPLPGG TGIPPPPPPL PGSVGVPPPP  700
PLPGGPGLPP PPPPFPGAPG IPPPPPGMGV PPPPPFGFGV PAAPVLPFGL  750
TPKKVYKPEV QLRRPNWSKF VAEDLSQDCF WTKVKEDRFE NNELFAKLTL  800
AFSAQTKTSK AKKDQEGGEE KKSVQKKKVK ELKVLDSKTA QNLSIFLGSF  850
RMPYQEIKNV ILEVNEAVLT ESMIQNLIKQ MPEPEQLKML SELKEEYDDL  900
AESEQFGVVM GTVPRLRPRL NAILFKLQFS EQVENIKPEI VSVTAACEEL  950
RKSENFSSLL ELTLLVGNYM NAGSRNAGAF GFNISFLCKL RDTKSADQKM 1000
TLLHFLAELC ENDHPEVLKF PDELAHVEKA SRVSAENLQK SLDQMKKQIA 1050
DVERDVQNFP AATDEKDKFV EKMTSFVKDA QEQYNKLRMM HSNMETLYKE 1100
LGDYFVFDPK KLSVEEFFMD LHNFRNMFLQ AVKENQKRRE TEEKMRRAKL 1150
AKEKAEKERL EKQQKREQLI DMNAEGDETG VMDSLLEALQ SGAAFRRKRG 1200
PRQVNRKAGC AVTSLLASEL TKDDAMAPGP VKVPKKSEGV PTILEEAKEL 1250
VGRAS*
```

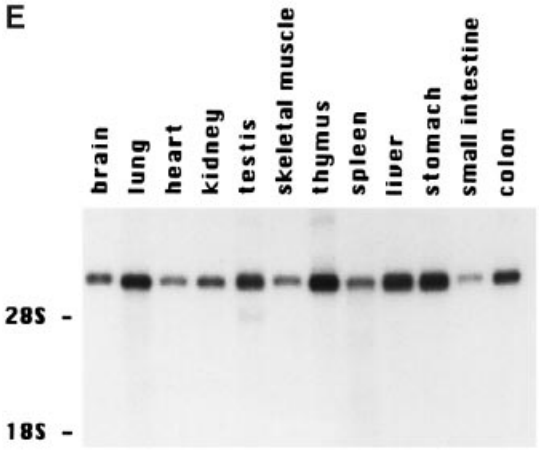

D

```
                                                                                    Two-hybrid clone
p140mDia    PGRGTRDKKK GRSPDELPAT GGDGGKHKKF LERFTSMRIK KEKEKPNSAH -------RNS SASYGDDPTA QSLQDISDE- QVLVLFEQML VDMNL----N   97
diaphanous    MSRHEKTKS STGGGLLDSL FGRPSKSKGG T---ISSGTL AHGGRPVSAD ---------N YVVPGVEDFE QYIQQLSVA- ELDAKFLEII EDMNI----P   81
Bni1p       NGKLSGDVPV SSQHARSHSM QSKYSYSKRN SSQASNKLTR QHTGQSHSAS SLLSQGSLTN LSKFTTPDGK IYLEMPSDPY EVEVLFEDIM YKRNIFQSLS  200

p140mDia    EEKQQPLREK DIVIKREMVS QYLHTSKAGM NQKESSR--- ---------- ------SAMM YIQELRSGLR DMHLL-SCLE SLRVSLNNNP VSWVQTFGAE  177
diaphanous  KDKREPLLAK SKEERQKMIM WHLK-GKNSL ERSANSR--- ---------- ----FEKPID YVEYLQNGEH STHKVYQQVE SLRVALTSNP ISWIKEFGVA  163
Bni1p       EDKQEALMGY SIEKKWLIVK QDLQNELKKM RANTTSSSTA -(90a.a.)- GDRTNRPPIH YVQRILADKL TS----DEMK DLWVTLRTEQ LDWVDAFIDH  376

p140mDia    GLASLLDILK R---LHDEKE ETSGNYDSRN QHEIIRCLKA FMNNKFGIKT ML--ETEEGI LLLVRAMDPA VPNMMIDAAK LLSALCILPQ PEDMNERVLE  272
diaphanous  GIGTIEKLLA R--------S KNNASYE-KI EFEAIRCLKA IMNNTWGLNV VLNPDQHSVV LLLAQSLDPR KPQTMCEALK LLASFCIVYE -RNGYEKVLR  253
Bni1p       QGHIAMANVL MNSIYKTAPR ENLTKELLEK ENSFFKGFRV LSMLSQGLYE FS--THRLMT DTVAEGLFST KLATRKMATE I--FVCML-- ----------  460

p140mDia    AMTERA--EM DEVERFQPLL DGL----KSG TSIALKVGCL QLINALITPA EELDFRVHIR SELMRL-GLH QVLQELREIT- ---ENEDMKV QLCVFDEQGD  361
diaphanous  AITTIAATSF KASERFRPIV DALFASDQQD PKRDLACHSL IFINTLTNTP TDLNFRLHLR CEIMRM-GLY DRLDEFTKIV EASNNENLQQ HFKIFNEIRE  352
Bni1p       --------EK KNKSRFEAVL TSL----DKK FRHGQNLHMI QNFKKMPQYF SHLTLESHLK IIQAWLFAVE QTLDGRGKMG SLVGASDEFK NGGGENAILE  548

p140mDia    ---------- EDFFDLKGRL PDIRMEMDD- -FGEVFQIIL NTVKDSKAEP HFLSILQHLL LVRNDYEARP QYYKLIEECV SQIVLHKNGT DPDF------  443
diaphanous  ---------- DDFEEFVQRF DNVTFNMDD- -ATDCFDVLK NLVTDTTSEP YFLSILQHLL YIRDDFYFRP AYYQLIEECI SQIVFHKGYC DPNF------  434
Bni1p       -(60a.a.)- LDDFNVKLEA NNKAFNVDLH DPLSLLKNLW DICKGTENEK LLVSLVQHLF L--------- SSSKLIEENQ NSSKLTKQLK LMDSLVTNVS  689

p140mDia    ------KCRH LQIDIERLVD QMIDKTKVEK SEAKATELEK KLDSELTARH ELQVEMKKME NDFEQKLQDL QGEKDALDSE KQQITAQKQD LEAEV-----  532
diaphanous  ------ENRN FNIDTSLLLD DIVEKAKA-K ESKRSEEYEK KIEQ------ ---------- ---------- ------LESA KQEAEAKAAH LEEKV-----  490
Bni1p       VASTSDEETN MNMATQRLYD AMQTDEVARR AILESRALTK KLEEIQAERD SLSEKLSKAE HGLVGQLEDE LHERDRILAK NQRV---MQQ LEAELEEL--  784

p140mDia    ---------S KLTGEVAKLS KELEDA---- ---------- --KNEMASLS AVVVAPSVSS SAAVPPAPPL PGDSGTVIPP PPPPPPP---          593
diaphanous  ---------- ---------- ---------- ---------- -KLMEANGVA APSPNKLPKV NIPMPPPPPG GGGAPPPPPP PMPGRA---          535
Bni1p       (40a.a.)-S LNSSEKANIQ KVLQDGLSR- (370a.a.)- SKLNNTDGAE DLSTQSSVLS SQPPPPPPP PPVPAKLFGE SLEKEK---         1262
```

the specificity of the interaction observed in the two-hybrid system. The specific association of p140mDia with the activated form of RhoA in both assays indicates that p140mDia may work as a downstream effector of Rho.

p140mDia is highly homologous to Drosophila diaphanous and is a formin-related protein

To obtain a full-length coding sequence, we sequentially screened two mouse brain cDNA libraries and a mouse embryo cDNA library. Six overlapping clones were isolated (Figure 3A). The composite cDNA sequence from clones 502, 503, 504 and E52 contains an open reading frame which encodes a protein of 1255 amino acids with a calculated mol. wt of 139 336 (Figure 3B). The Rho-binding region defined by clone 50 cDNA is located in the N-terminal portion (amino acids 63–260). Between amino acid 571 and 737, there is a region with 14 repeats of polyproline stretches. The repeats are characterized by a motif, IPPPPPLPG, or similar sequences. Five repeats share this motif exactly, while there exist variations, including the extension of the polyproline by one or three prolines. The disruption of the polyproline at position 4 by alanine or serine is also seen in two repeats. We compared the amino acid sequence, excluding polyproline sequences, of this protein with other sequences in the databases using the BLASTP program (Stephen *et al.*, 1990). The search revealed one highly homologous protein, *Drosophila* diaphanous, required for cytokinesis (Castrillon and Wasserman, 1994). Diaphanous also contains polyprolines in the middle and shows 30 and 39% identity upstream and downstream of the polyproline region to the respective regions of p140mDia (Figure 3C). Several related proteins have also been identified. These proteins include Bni1p of *Saccharomyces cerevisiae* (DDBJ/EMBL/GenBank L31766), mouse formin (Woychick *et al.*, 1990), *Drosophila* cappuccino (Emmons *et al.*, 1995), fus1p of *Schizosaccharomyces pombe* (Petersen *et al.*, 1995) and FigA of *Aspergillus nidulans* (Marhoul and Adams, 1995). These proteins belong to a family of formin-related proteins, and contain the polyproline region and the highly conserved portion in the C-terminal region which Castillon and Wasserman (1994) designated as FH1 and FH2 domains, respectively. Additionally, distant homology is present in sequences from the polyproline region to the C-terminus of all these molecules. Only diaphanous is highly homologous to p140mDia also in the N-terminal part, which includes the Rho-binding domain. p140mDia also shows weak but significant homology in the entire sequence, including the Rho-binding region, to Bni1p (Figure 3D), which is involved in yeast cell budding. Northern blot analysis revealed that a major 6.3 kb transcript for this novel Rho-binding protein was expressed ubiquitously in all mouse tissues examined (Figure 3E).

p140mDia binds to profilin in vitro

An actin-binding protein, profilin, is known to bind also to poly-L-proline (PLP) *in vitro* (reviewed by Machesky and Pollard, 1993) and can be purified selectively by the use of PLP–Sepharose affinity chromatography (Tanaka and Shibata, 1985). Hence, we speculated that p140mDia might bind to profilin. Recently, Reinhard *et al.* (1995) reported that two polypeptides, VASP and an 81 kDa fragment of an unidentified 160 kDa protein, bound to profilin–agarose and were eluted by PLP solution. We noticed that the sequences of amino acids 731–769 and 1128–1152 of p140mDia were almost identical to the partial amino acid sequences of the fragment of this 160 kDa protein. We therefore examined whether p140mDia can bind to profilin and whether the binding of p140mDia to profilin is dependent on Rho, because the fragment isolated by Reinhard *et al.* (1995) corresponds to the C-terminal part of p140mDia. As shown in Figure 4, p140mDia in Swiss 3T3 cell lysates was quantitatively precipitated by the addition of profilin–agarose, while no precipitation was seen with bovine serum albumin (BSA)–agarose. This interaction was not affected by the addition of exogenous RhoA. It also was not affected by the addition of Rac1 or Cdc42Hs or by the addition of GTPγS (data not shown).

Co-localization of RhoA, p140mDia and profilin in membrane ruffles of motile cells

The intracellular distribution of p140mDia was first examined in Swiss 3T3 cells (Figure 5A and B). Although the majority of fluorescence obtained by affinity-purified anti-p140mDia antibody (AP50) was localized to the thicker regions of the cells, prominent fluorescence was observed in the spreading lamellae, where fine actin ribs are developed. No association of p140mDia with focal adhesions and stress fibers was observed. In mitotic cells, p140mDia was associated with the plasma membrane rather homogeneously. However, in some mitotic cells, p140mDia was concentrated in the cleavage furrow and appeared as a ring-like structure (Figure 5C and D).

The subcellular localization of p140mDia, profilin and RhoA was then studied in HT1080 human fibrosarcoma cells. In addition to perinuclear staining, the peripheral

Fig. 3. Structure of p140mDia. (**A**) Schematic representation of the isolated cDNA clones. An open reading frame is indicated by a dotted box on the composite cDNA. Two nucleotide substitutions, T→C at nucleotide 87 and C→T at nucleotide 2229, are noted in 503 and E73 cDNA, respectively. These substitutions cause no change in coded amino acids. Library a, b and c refer to the mouse brain libraries 936309 (Stratagene) and ML3000a (Clontech) and the mouse embryo library (Nakagawa *et al.*, 1996), respectively. A nine amino acid insertion was found in clone E73 cDNA. (**B**) Deduced amino acid sequence of p140mDia. A sequence encoded by the two-hybrid plasmid, pVP-cl.50, is indicated by a bold underline. A repetitive polyproline region is indicated by a broken line and an FH2 domain is indicated by a thin underline. An arrowhead indicates the position of a nine amino acid insertion, TLKRLMADE, found in E73. The accession number of the nucleotide sequence in DDBJ/EMBL/GenBank is U96963. (**C**) Schematic presentation of p140mDia and other formin-related proteins. The identity was calculated by the ratio of the number of the identical amino acids to that of the corresponding amino acids of p140mDia and is expressed as a percentage in each indicated region. Comparison is made against *Drosophila* diaphanous (DDBJ/EMBL/GenBank accession No. U11288), *S.cerevisiae* Bni1p (DDBJ/EMBL/GenBank accession No. L31766), mouse formin IV (DDBJ/EMBL/GenBank accession No. X62379) and *Drosophila* cappuccino (DDBJ/EMBL/GenBank accession No. U34258). *, no significant homology to p140mDia found in the N-terminal regions of formin and cappuccino. (**D**) Alignment of N-terminal amino acid sequences between p140mDia, diaphanous and Bni1p. Identical amino acids between two or three sequences are shown by white letters on a black background. The coding region of the initial two-hybrid plasmid, pVP-cl.50, is indicated by a stippled arrow. (**E**) Northern blot analysis of p140mDia expression in various mouse tissues.

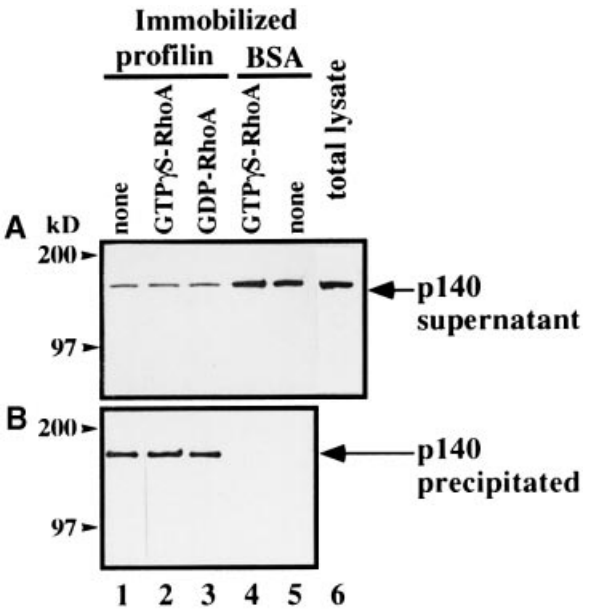

Fig. 4. Interaction of p140mDia and profilin *in vitro*. Swiss 3T3 cell lysates were incubated with agarose beads conjugated either with profilin or with BSA in the presence or absence of either the GTPγS- or GDP-bound form of bacterially expressed RhoA, and associated proteins were precipitated. Half of the proteins precipitated with beads (**B**) or one-tenth of the remaining supernatants (**A**) were subjected to the Western blotting with anti-p140mDia.

lamellae of motile cells were enriched with the fluorescent signals for all three proteins. The signals were abolished by prior absorption of the antibodies with the respective antigens (Figure 6). This pattern of profilin distribution is consistent with the pattern demonstrated in the previous study of rat fibroblasts and BHK cells (Buß *et al.*, 1992; Rothkegel *et al.*, 1996). Using these antibodies and phalloidin, localization of the three molecules and F-actin were compared by dual immunofluorescence. HT1080 cells extend massive ruffles around their periphery, which were strongly stained with phalloidin (Figure 7B). Some p140mDia was detected in these ruffles, and was concentrated most notably at their tips (Figure 7A). Dual fluorescence with anti-p140mDia and anti-profilin antibodies revealed co-localization of the two molecules in membrane ruffles (Figure 7C and D), which is shown more clearly by confocal microscopy (Figure 7C′ and D′). Moreover, double immunofluorescence images produced by the polyclonal anti-RhoA antibody and anti-profilin antibody revealed nearly identical patterns at the membrane ruffles of the cells (Figure 7E and F, E′ and F′), suggesting that p140mDia, profilin and RhoA are associated in these highly motile structures.

We also examined the localization of p140mDia, RhoA and profilin in sMDCK2 cells which stably express myc-tagged RhoA and which rapidly extend membranes in response to 12-*O*-tetradecanoylphorbol-13-acetate (TPA) (Takaishi *et al.*, 1995). Both p140mDia and myc-RhoA were distributed rather homogeneously in the cytoplasm of resting cells. After stimulation by TPA for 15 min, a portion of myc-RhoA moved to the peripheral membrane ruffles, where p140mDia as well as profilin was co-localized (data not shown). Because the TPA-induced membrane extension and ruffles of these cells occur in a Rho-dependent manner (Takaishi *et al.*, 1995), these results demonstrate the co-localization of the three proteins, RhoA, p140mDia and profilin, in a Rho-dependent structure.

Activation-dependent clustering of RhoA, p140mDia and profilin around fibronectin-coated beads

Recent studies indicate that integrin ligation by either FN- or anti-integrin antibody-coated beads recruits RhoA and p190RhoGAP-B to the plasma membrane beneath the beads (Burbelo *et al.*, 1995b; Miyamoto *et al.*, 1995). We therefore examined if p140mDia and profilin are also recruited to the plasma membrane around FN-coated beads and co-localize with RhoA. As shown in Figure 8A and C, we confirmed that RhoA was recruited efficiently by the FN-coated beads and clustered around the beads. Much less accumulation was found around the PLL-coated beads (data not shown). Under these conditions, p140mDia also accumulated around the FN-coated beads and exactly co-localized with RhoA (Figure 8B). Co-localization of profilin was also noted (Figure 8D). To test if the recruitment of p140mDia is dependent on Rho, we inactivated endogenous Rho by microinjecting C3 exoenzyme and then carried out the bead assay on the injected cells. As shown in Figure 8E–H, no recruitment of p140mDia and RhoA was found in the C3 exoenzyme-injected cells, indicating that activation of Rho is required for the recruitment of these molecules to phagocytic cups around the beads.

Overexpressed p140mDia induces homogeneous fine actin filaments

Finally, we examined the effect of p140mDia overexpression on the actin cytoskeleton in COS-7 cells. Cells overexpressing p140mDia showed the homogeneous anti-p140mDia staining with clear cell contours (Figure 9A), indicating that some of the p140mDia accumulated on the plasma membrane. This membrane association was a persistent finding in transfected cells, although a portion of p140mDia formed aggregates in the cytoplasm of cells expressing a very high level of p140mDia or co-expressing Val14-RhoA (data not shown). Double staining with phalloidin revealed reduction in stress fibers and enhancement of fine F-actin staining in almost all cells showing p140mDia overexpression (Figure 9B and B′). The homogeneous distibution of fine F-actin was observed even after p140mDia was co-expressed with C3 exoenzyme. Expression of C3 exoenzyme alone almost abolishes F-actin staining in COS-7 cells (see examples of C3 exoenzyme phenotype of COS-7 cells; arrowheads in Figure 9D and D′). When p140mDia and C3 exoenzyme were expressed together at a higher level, the cells showed homogeneous F-actin staining (arrows in Figure 9C and D, and Figure 9D′) similar to that obeserved in cells overexpressing p140mDia alone. The induction of fine actin filaments was persistently observed in all cells that expressed a high level of p140mDia and C3 exoenzyme, indicating that overexpressed p140mDia can promote actin polymerization in the absence of Rho activity. To evaluate the nature of F-actin induced by overexpressed p140mDia, we extracted the cells with 0.1% Triton in the presence of phalloidin before fixation. Because this procedure extracted most of the expressed p140mDia, we

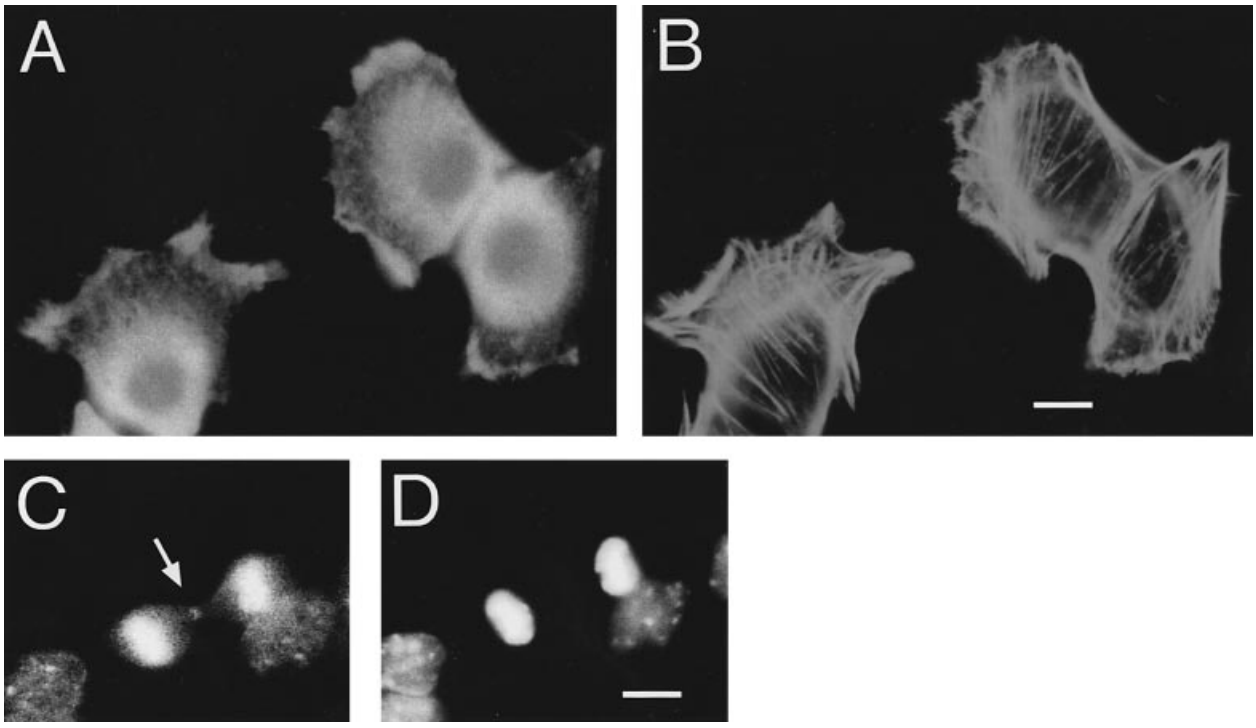

Fig. 5. Localization of p140mDia in spreading and dividing Swiss 3T3 cells. (**A** and **B**) Concentration of p140mDia in spreading lamellae of Swiss 3T3 cells. Cells were cultured and fixed as described in Materials and methods. The cells were stained with anti-p140mDia antibody (AP50) (A) simultaneously with phalloidin (B) to detect F-actin and photographed. Bar represents 10 μm. (**C** and **D**) Concentration of p140mDia in the cleavage furrows of dividing cells. Logarithmically growing cells stained with anti-p140 antibody (C) and simultaneously stained with DAPI (D) were photographed by a standard fluorescence microscope. A small ring-like structure is observed with anti-p140mDia staining in the cleavage furrow in (C) (arrow). Nuclear staining in (C) is due to the leakage of the strong DAPI staining in (D). Bar, 10 μm.

examined F-actin staining only in the cells containing overexpressed p140mDia as insoluble aggregates. F-actin staining remained homogeneous in these cells (data not shown).

Discussion

p140mDia is a novel target protein of Rho

This two-hybrid screening initially was aimed at isolating a novel exchange factor for RhoA. Asn17-Cdc42Hs binds strongly to a *dbl* oncogene product bearing a catalytic domain for the GDP/GTP exchange of Cdc42Hs and RhoA (Hart *et al.*, 1994). Indeed, Asn19-RhoA and its C-terminal truncated form interact with Dbl far more strongly than does wild-type RhoA in a two-hybrid system (N.Watanabe, unpublished results). However, we did not obtain any proteins with Dbl homology in this screening. This may be due to the short size of the cDNA in the library used in the two-hybrid screening, which we found up to ~650 bp. Hart *et al.* (1994) reported that the minimum Dbl domain consisted of 260 amino acids. By this screening, we have isolated the Rho-binding domain of p140mDia instead. Strong interaction of p140mDia with Val14-RhoA in the two-hybrid system and its specific association with the GTPγS-bound form of RhoA *in vitro* indicate that p140mDia is a downstream target molecule of Rho. Among the effectors of the Rho family of GTPases reported thus far, PKN, rhophilin and rhotekin possess a conserved Rho-binding motif (Reid *et al.*, 1996), and PAK, STE20 and WASP of Rac/Cdc42 effectors share a conserved Rac/Cdc42-binding motif (Burbelo *et al.*, 1995a; Symons *et al.*, 1996). However, p140mDia does not show any significant homology to other effectors of Rho.

p140mDia is a mammalian homolog of Drosophila diaphanous

Structural elucidation and a comparison of p140mDia with sequences in databases has revealed that p140mDia belongs to a family of formin-related proteins. The functions of all of these proteins are related to the regulation of cell structure and polarity. *Drosophila* diaphanous is required for cytokinesis. Bni1p is involved in yeast bud formation. Formin is a product of a mouse gene for proper limb pattern formation. Cappuccino is essential for the polarity of *Drosophila* egg formation. Fus1 of *S.pombe* is required for cell wall fusion during conjugation. These proteins share homology in sequences extending from the polyproline region to the C-terminus, while the N-terminal regions are divergent. For example, formin is spliced in its N-terminal region, yielding variants bearing N-termini of quite different isoelectric points (Jackson-Grusby *et al.*, 1992). Hence, it appears that formin-related molecules have preserved the C-terminal half during evolution, which suggests that this region is associated with functions common to all of these molecules. In particular, the polyproline region (FH1) and the highly-conserved FH2 domain may serve as domains which interact with some cytoskeletal elements. In contrast, the divergent N-termini may provide the differentially evolved function for each

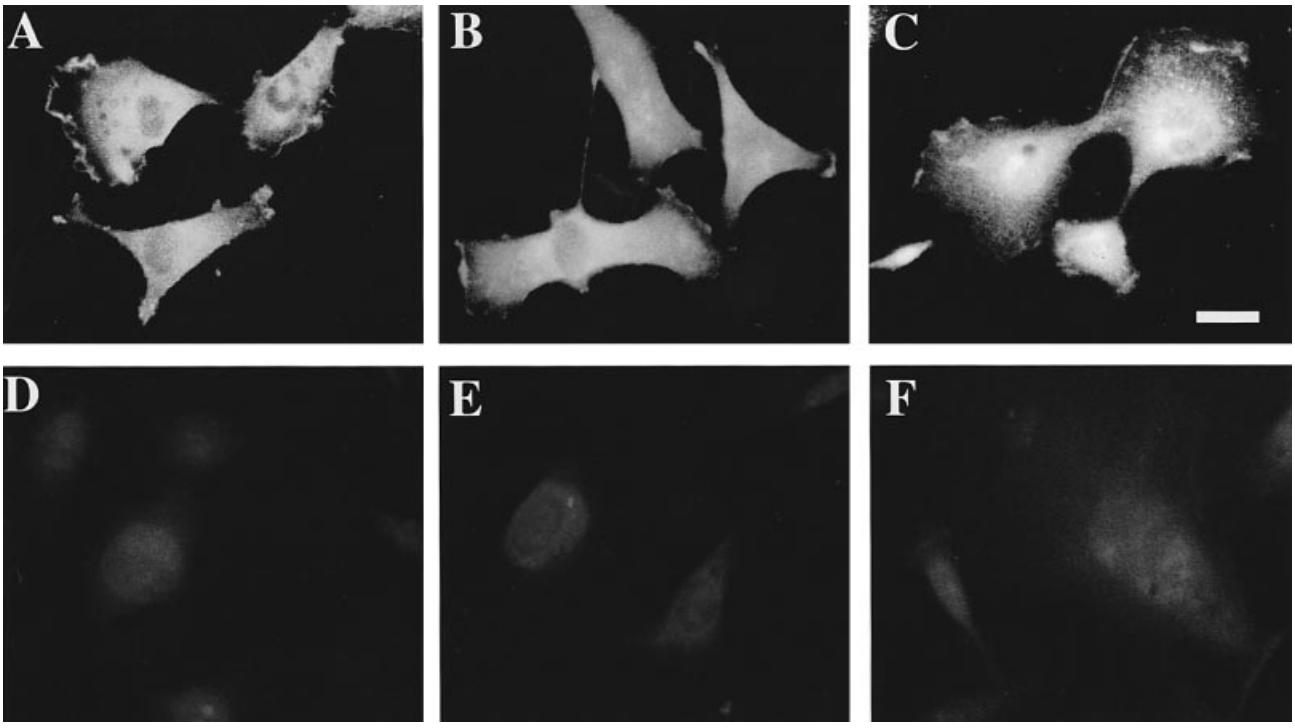

Fig. 6. Intracellular localization of p140mDia, profilin and RhoA in HT1080 human fibrosarcoma cells. Cells stained with anti-p140mDia antibody (AP50) (**A**), monoclonal anti-profilin antibody (2H11) (**B**) or polyclonal anti-RhoA antibody (**C**) were photographed by a standard fluorescence microscope. In (D–F), antibody preparations pre-absorbed with the respective antigen as described in Materials and methods were used. Fluorescence signals with antibody-depleted AP50 (**D**), antibody-depleted 2H11 (**E**) and antibody-depleted polyclonal anti-RhoA antibody preparation (**F**) were photographed. Bar, 25 μm.

molecule. p140mDia is highly homologous only to diaphanous in the N-terminus, which includes the Rho-binding domain. Relative enrichment of p140mDia in the cleavage furrow of some dividing cells may support the functional conservation between p140mDia and diaphanous. Taken together, these data suggest that p140mDia is a mammalian homolog of *Drosophila* diaphanous. In addition, Bni1p, which retains distant homology to p140mDia also in the Rho-binding domain, may be a yeast homolog of p140mDia.

p140mDia, a ligand for profilin

Castillon and Wasserman (1994) noted the similarity between the mutant phenotypes of diaphanous and chickadee, a *Drosophila* profilin, and suggested the possibility that diaphanous binds to chickadee through its polyproline motifs. Disruption of the profilin gene results in a cytokinesis-defective phenotype in *Drosophila* (Verheyen and Cooley, 1994), *S.pombe* (Balasubramanian *et al.*, 1994) and *Dictyostelium* (Haugwitz *et al.*, 1994). Similarly, inactivation of Rho by C3 exoenzyme also prevents the formation and maintenance of the cleavage furrow in dividing oocytes (Mabuchi *et al.*, 1993). Moreover, both Rho (Aullo *et al.*, 1993) and profilin (Theriot *et al.*, 1994) are required for the movement of intracellularly infected *Listeria monocytogenes.* Hence, there are certain cellular processes requiring all three proteins, Rho, diaphanous and profilin. Here, we have demonstrated that intact p140mDia can bind to profilin *in vitro*, and its distribution *in vivo* largely overlaps with that of profilin in cells. These results strongly indicate that profilin associates physically with p140mDia not only *in vitro* but also *in vivo*. VASP, showing a similar *in vivo* co-localization to profilin, has been the only ligand of profilin identified thus far among many polyproline-containing proteins (Reinhard *et al.*, 1995). VASP and p140mDia appear to be two major profilin ligands in cells, because they were the two major proteins isolated by profilin–agarose affinity chromatography (Reinhard *et al.*, 1995). Recently, another polyproline protein, WASP, was identified as a putative effector for Cdc42Hs (Symons *et al.*, 1996). While overexpression of WASP induces actin polymerization, no link between WASP and profilin has been reported yet.

Rho-dependent targeting of profilin: possible mechanism for focal actin reorganization

The present study has examined extensively the subcellular localization of endogenous RhoA, p140mDia and profilin, and has shown that the three proteins are co-localized in membrane ruffles, especially at the tip of ruffles, of motile cells. Co-localization of these three proteins was also observed around the phagocytic cups induced by FN-coated beads. It is noteworthy that the co-localization in both structures is dependent on the action of Rho. Firstly, on TPA stimulation, sMDCK2 cells rapidly extend their membranes with fine ruffles at their edges, where myc-RhoA is co-localized with p140mDia and profilin. Microinjection of C3 exoenzyme or Rho-GDI abolished membrane extension and ruffle formation of these cells (Takaishi *et al.*, 1995). Secondly, the recruitment of RhoA and p140mDia around FN-coated beads is also abolished by prior injection of C3 exoenzyme. These results strongly suggest that p140mDia and profilin are recruited to these dynamic membrane structures by the action of Rho.

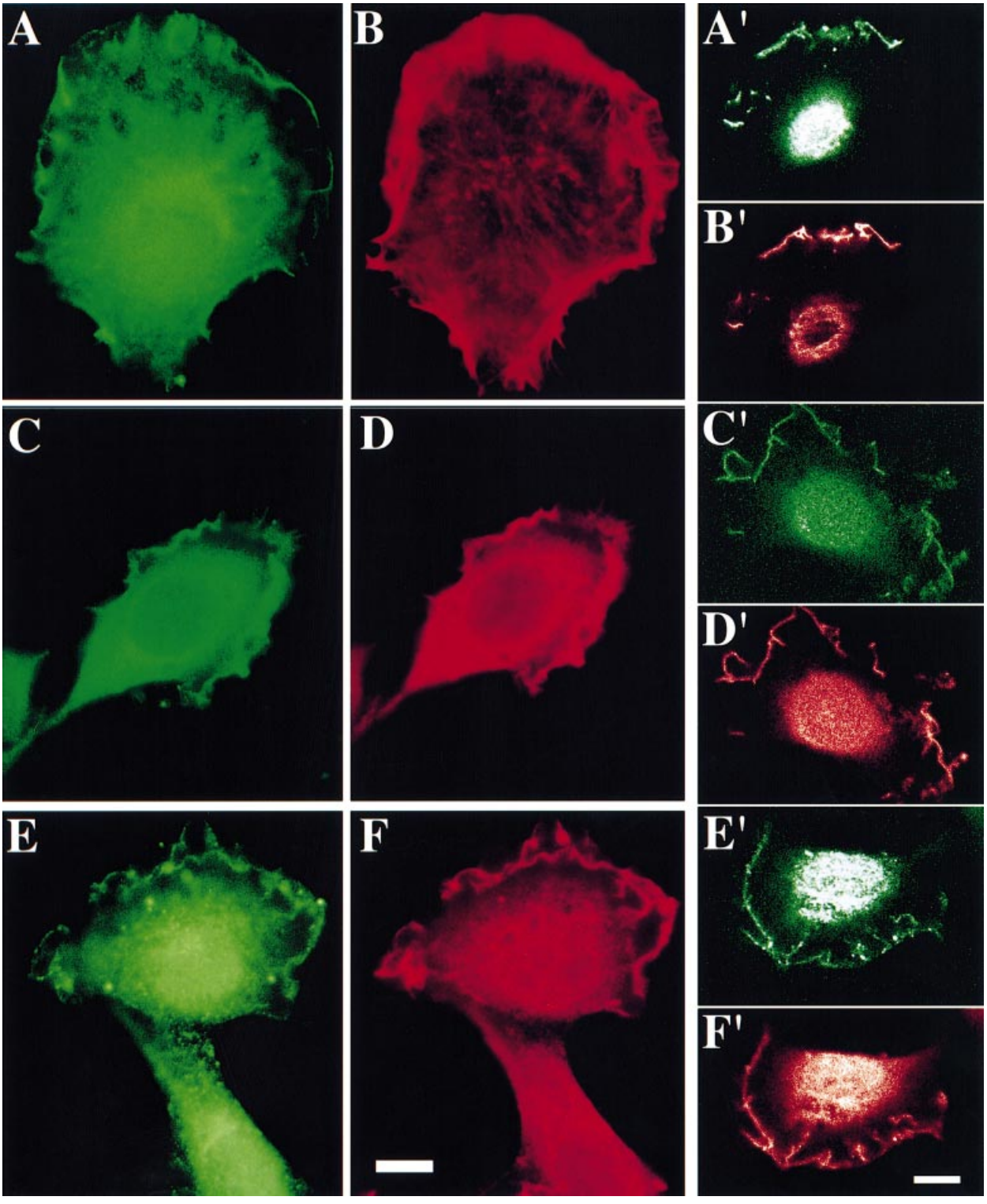

Fig. 7. Co-localization of RhoA, p140mDia and profilin in membrane ruffles of HT1080 cells. Cells simultaneously stained with either anti-p140mDia antibody (AP50) (**A** and **A′**) and phalloidin (**B** and **B′**), anti-p140mDia antibody (AP50) (**C** and **C′**) and mouse monoclonal anti-profilin antibody 2H11 (**D** and **D′**) or polyclonal anti-RhoA antibody (**E** and **E′**) and mouse monoclonal anti-profilin antibody 2H11 (**F** and **F′**) were photographed by a standard fluorescence microscope (A–F) or by a confocal laser scanning microscope (A′–F′). A′–F′ demonstrate the dual fluorescence sections close to the top of the cells. Bar, 10 μm.

As Grinnel and Geiger (1986) noted, the phagocytic membranes around the FN-coated beads are morphologically similar to the membrane ruffles seen in the edges of cultured cells. Recently, similar Rho-dependent membrane folding was reported at the entry of *Shigella* into epithelial cells (Adam *et al.*, 1996). Rho is also required for HGF- and TPA-induced membrane ruffles in KB cells, which are morphologically different from Rac-dependent, insulin-induced ruffles (Nishiyama *et al.*, 1994). All of these structures are associated with dynamic

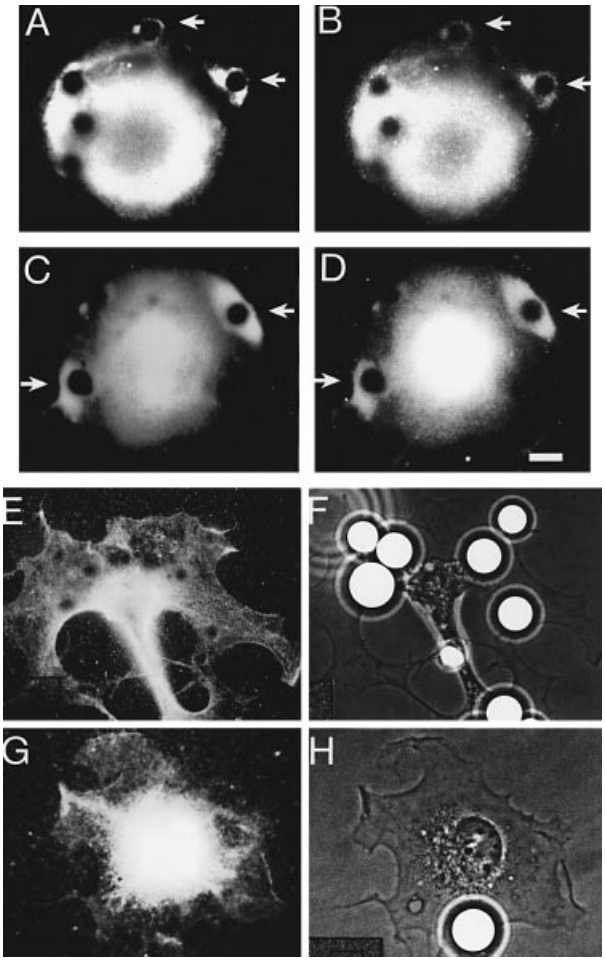

Fig. 8. RhoA, p140mDia and profilin cluster around FN-coated beads in a Rho-dependent manner. (A–D) Co-clustering of RhoA, p140mDia and profilin. Trypsinized Swiss 3T3 cells were plated on FN-coated glass coverslips and grown for 2 h. The cells were then incubated with latex beads coated with FN for 15 min. The cells were fixed and stained with anti-RhoA antibody (26C4) (**A** and **C**) and simultaneously with anti-p140mDia antibody (AP50) (**B**) or with anti-profilin serum (**D**). Arrows indicate the position of the FN-coated beads which induced typical accumulation of each molecule. (E–H) Absence of clustering in C3 exoenzyme-injected cells. C3 exoenzyme (150 ng/μl) with a marker was microinjected into Swiss 3T3 cells grown for 2 h on FN-coated glass coverslips. After 20 min, the cells were incubated with FN-coated beads for 15 min and fixed. The injected cells stained with anti-p140mDia (AP50) (**E**) or with anti-RhoA antibody (26C4) (**G**) are shown. The beads attached to the same cells in (E) and (G) are shown by the phase-contrast images (**F** and **H**). Bars, 10 μm.

actin polymerization, and appear to be highly related in view of the morphological similarities and the functional connections with Rho. Profilin is also thought to be involved in actin polymerization beneath the dynamic plasma membranes. It is transiently translocated to the plasma membrane of stimulated platelets and leukocytes (Hartwig *et al.*, 1989) and is concentrated in the ruffling membranes of locomoting fibroblasts (Buß *et al.*, 1992). Since a small amount of profilin can promote extensive actin filament assembly from the G-actin–thymosin β4 precursor pool (Pantaloni and Carlier, 1993), the targeting of profilin has been thought to be important in the enhanced actin polymerization at these membranes. One candidate responsible for this targeting is PIP_2 (Hartwig *et al.*, 1989). While the synthesis of PIP_2 can be stimulated by Rho (Chong *et al.*, 1994), it is not known yet whether Rho activates PIP_2 synthesis locally in the above membranes. The identification of p140mDia suggests that Rho and p140mDia are the long-sought targeting vehicles for profilin, and that the p140mDia–profilin complex targeted by Rho possibly acts on focal actin polymerization. This idea would be in agreement with the results of transient p140mDia expression in COS-7 cells. The overexpressing cells showed the diffuse staining for p140mDia and the enhanced fine actin filament assembly in the entire cell. Co-expression with C3 exoenzyme did not alter this diffuse localization of p140mDia. These results showed that overexpressed p140mDia was not regulated by Rho and was distributed evenly in the cell. The homogeneous distribution of the induced F-actin in both transfectants may thus reflect the loss of a precise mechanism for its localization.

On the bases of these observations, we have devised a model for a p140mDia-mediated action of Rho as depicted in Figure 10. In this scheme, Rho is activated locally and recruits p140mDia–profilin beneath a specific site of the plasma membrane. The locally increased concentration of profilin then promotes actin polymerization. It is likely that multiple profilin molecules bind simultaneously to a single p140mDia. Since it has been shown that profilin bound to actin exposes the PLP-binding site (Tanaka and Shibata, 1985; Schutt *et al.*, 1993), the profilin–actin complex may also bind to p140mDia. Whether p140mDia influences profilin-catalyzed actin polymerization is an interesting question to be investigated. PIP_2 possibly also works cooperatively in this context.

It is well known that microinjection of Rho induces focal adhesion and stress fiber formation in cultured fibroblasts (Ridley and Hall, 1992). However, neither Rho nor p140mDia has ever been observed to be concentrated at focal adhesions or stress fibers (Adamson *et al.*, 1992; Takaishi *et al.*, 1995; this study). Recent reports showed that Rho-induced focal adhesion and actin polymerization are inhibited differentially by staurosporine and cytochalasin D (Nobes and Hall, 1995). We presume, therefore, that two or more Rho effectors work in combination to induce Rho effects and that some may work at earlier steps before the final structures are stabilized. Based on the experiments on molecular clustering around the FN-coated beads (similar to experiments employed in this study), Miyamoto *et al.* (1995) proposed a multi-step model for focal complex formation.

In summary, we have identified p140mDia as a new Rho target. It provides a direct molecular link between Rho and profilin, which have been characterized separately as a regulator for the actin cytoskeleton. The functions and subcellular localization of the three molecules suggest that they work cooperatively in actin reorganization beneath the dynamic plasma membranes. Future studies will reveal how these molecules work together with other Rho effectors and the actin cytoskeleton in dynamic movement of the plasma membranes.

Materials and methods

Plasmids

pGEX-RhoA has been described previously (Watanabe *et al.*, 1996). pGEX-Rac1 and pGEX-Cdc42Hs were gifts of Y.Takai. pBTM-RhoA

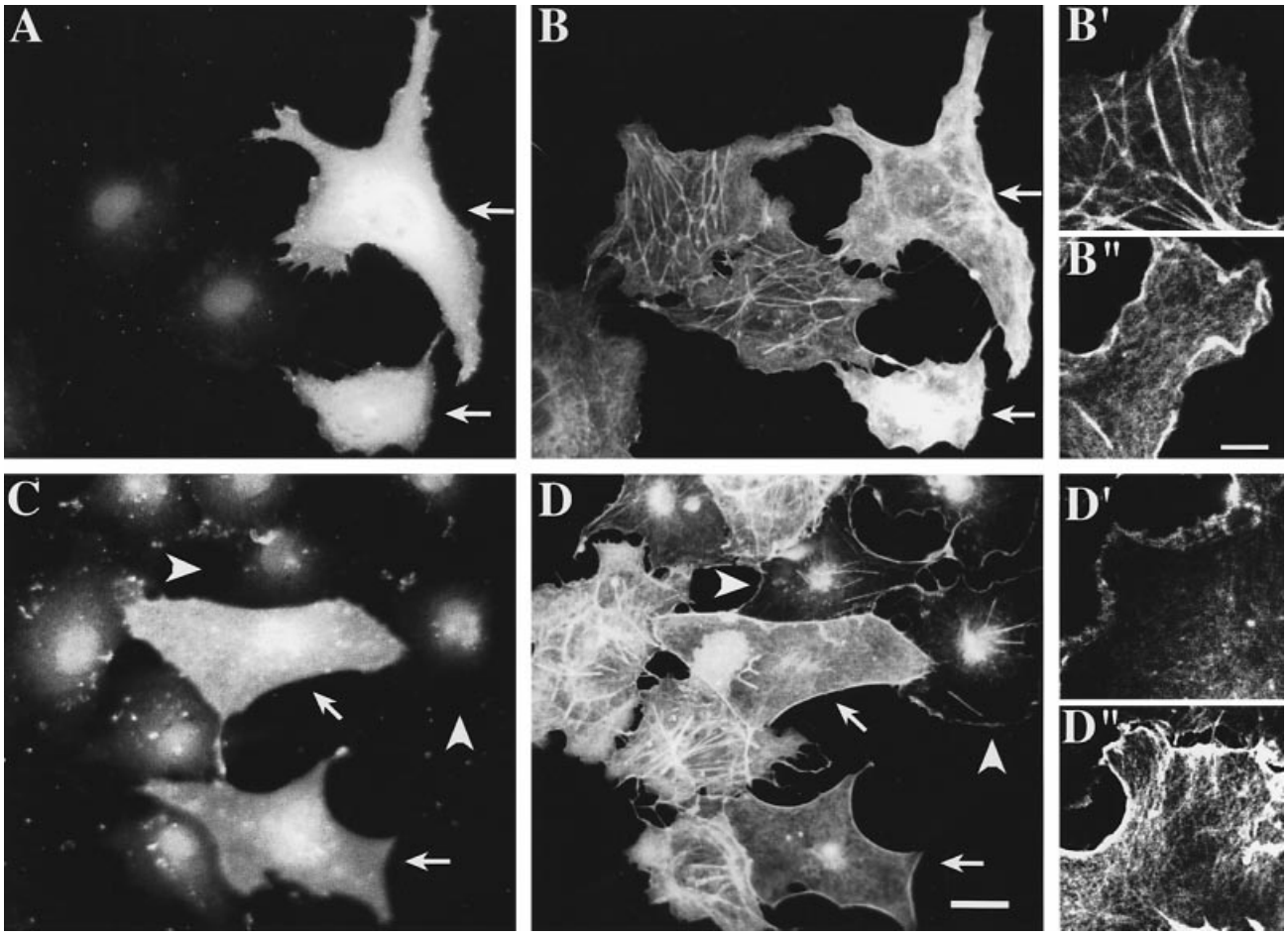

Fig. 9. Transient expression of p140mDia in COS-7 cells. COS-7 cells on 3.5 cm culture dishes were transfected with an expression vector of p140mDia (pCMX-p140, 1 μg) alone (A, B, B′ and B″) or with the combination of 1 μg of pCMX-p140 and 0.1 μg of pEFBOS-C3 (C, D, D′ and D″). Cells were fixed and stained simultaneously for p140mDia (**A** and **C**) and for F-actin with phalloidin (**B**, **B′**, **B″** and **D**, **D′**, **D″**). Arrowheads in (D) indicate the cells exhibiting the typical F-actin staining of C3 exoenzyme-expressing COS-7 cells. Note that in these cells, p140mDia expression does not exceed the endogenous levels (arrowheads in C). Arrows indicate p140mDia-overexpressing cells (A–D). The COS-7 cells overexpressing p140mDia with C3 exoenzyme consistently show homogeneous F-actin staining similar to the cells indicated by arrows in (D). Bar, 25 μm. (B′, B″, D′ and D″) Detailed F-actin staining of control cells (B′), cells overexpressing p140mDia alone (B″), C3 exoenzyme-expressing cells (D′) and cells overexpressing p140 mDia with C3 exoenzyme (D″) were studied by a confocal laser scanning microscope, and optical sections close to the bottom of cells in each study are shown. Bar, 10 μm.

was prepared as described previously (Watanabe *et al.*, 1996). To generate Val14 and Asn19 mutations on RhoA, the *Bam*HI–*Eco*RV fragment of the pGEX-RhoA encoding the RhoA N-terminus was ligated into pBluescript (Stratagene), and mutagenized according to the method of Kunkel (1985). The corresponding wild-type fragment of pGEX-RhoA was then replaced by each mutagenized fragment, and the *Bam*HI–*Eco*RI fragments encoding the full-length coding region of these mutant RhoAs were ligated into pBTM116 to yield pBTM-Val14-RhoA and -Asn19-RhoA, respectively. The C-terminal deletion of these mutants at Ala181 (pBTM-Val14-RhoAΔC and -Asn19-RhoAΔC) was prepared as described previously (Reid *et al.*, 1996). The *Bam*HI–*Bam*HI fragment of pGEX-Cdc42Hs was also ligated into pBTM116. All the other plasmids used in the two-hybrid system, including the cDNA library, were kindly provided by Stan Hollenberg, Rolf Sternglanz, Stan Fields and Paul Bartel (Vojtek *et al.*, 1993).

Yeast two-hybrid screening

The yeast L40 strain harboring pBTM-Asn19-RhoAΔC was transformed with pVP16 fused with a mouse embryo cDNA library. Initial transformation yielded 2.2×10^7 clones, which were amplified seven times during the 6 h culture before spreading on His (–) plates. Among 1.5×10^8 transformants, 978 clones were isolated as His^+ and $LacZ^+$, and 220 clones were cured from the bait plasmid. Interactions with other proteins were evaluated by mating with yeast strain AMR70 harboring various test baits. Clones interacting with a negative control, lamin, were eliminated. When the remaining 55 clones were mated to AMR70 strains bearing LexA fused to various RhoA mutants, all of them showed an interaction that was strongest with Val14-RhoA, less strong with RhoAΔC and wild-type RhoAΔC, weak with Asn19-RhoA and almost negligible with wild-type RhoA. The plasmids recovered from these clones were identical. A representative clone, clone 50, was used for further analysis. To confirm the specificity of the interactions in a two-hybrid system, a pVP16 plasmid recovered from yeast clone 50 (pVP-cl.50) was co-transformed into L40 with various pBTM116 plasmids. These transformants were plated as patches on selective medium, transferred on cellulose filters, and β-galactosidase activity was assayed as described (Vojtek *et al.*, 1993).

cDNA screening

Two mouse brain libraries (936309 in λZAP II, Stratagene, and ML3000a in λgt-10, Clontech) were screened with the ^{32}P-labeled 0.6 kb cDNA insert of pVP-cl.50. One positive clone, clone 502, and two positive clones, clones 503 and 504, were obtained from the former and the latter library, respectively. Using the 5′ part of 504 and the 3′ part of 503 as probes, clones E51, E52 and E73 were isolated from a mouse embryo library (Nakagawa *et al.*, 1996). Nucleotide sequence was determined using the dideoxy chain termination method.

Northern blot analysis

$Poly(A)^+$ RNA was prepared from several tissues of adult mice using oligo(dT) latex beads according to the standard procedure (Sambrook *et al.*, 1989). Six μg of each $poly(A)^+$ RNA was separated on a 1.0%

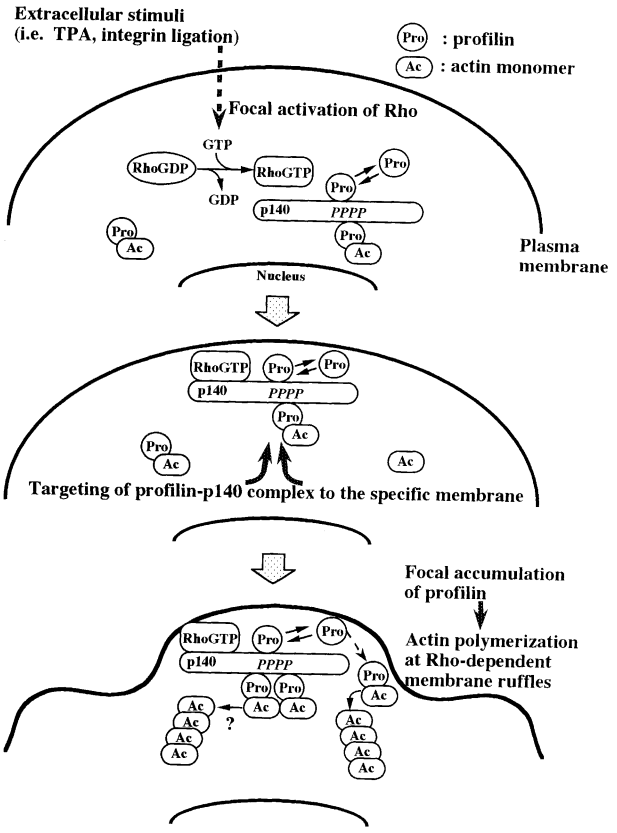

Fig. 10. A model for p140mDia-mediated reorganization of the plasma membrane and the actin cytoskeleton. The upper figure shows a resting cell where Rho has just been activated. The binding between p140mDia and profilin is not regulated by Rho and is constitutively present in this model. Upon binding of RhoGTP, p140mDia is recruited to the specific site of plasma membrane with profilin by an unidentified mechanism. In the lower figure, the focally elevated concentration of profilin promotes actin polymerization. Profilin works on actin either dissociated from p140mDia or attached to p140mDia.

agarose gel containing 2.1% formaldehyde, and transferred to a Biodyne A filter (Pall BioSuport, NY). The filter was then hybridized with the ^{32}P-labeled 0.6 kb cl.50 cDNA. The filter was washed finally with 0.4× SSC and 0.1% SDS at 65°C, and subjected to autoradiography.

Antibodies

Anti-p140mDia antibody was prepared as follows. The *Bam*HI and *Eco*RI sites of pVP-cl.50 flanking the cDNA insert were used to ligate cl.50 cDNA into pQE11 (QIAGEN) and pGEX-3X (Pharmacia) vectors. His_6-tagged cl.50 was expressed in *E.coli* JM109 strain and was purified with Ni-NTA resin (QIAGEN) according to the manufacturer's protocol. The purified protein mixed with Freund's adjuvant was injected into rabbits, and anti-p140mDia antiserum was raised. The antibody was then affinity purified using GST–cl.50 fusion protein immobilized on nitrocellulose membranes essentially as described (Reinhard *et al.*, 1992). Briefly, inclusion bodies containing GST–cl.50 were isolated from *E.coli* and solubilized in Laemmli's buffer. The solubilized proteins were separated by SDS–PAGE and transferred to the nitrocellulose membranes. A band of GST–cl.50 was excised as a strip, and antibodies absorbed to this strip were eluted at 4°C successively with 100 mM glycine–HCl buffer (pH 2.3), 100 mM monoethanolamine buffer (pH 11.5) and 100 mM glycine–HCl containing 10% 1.4-dioxane (pH 2.5). The eluates were neutralized immediately with 0.25 vol. of 250 mM sodium phosphate buffer (pH 8.8 for the first and third eluates and pH 7.0 for the second eluate). These eluates were combined and used as the affinity-purified antibody, AP50.

Polyclonal rabbit anti-profilin antibody was described previously (Buß *et al.*, 1992) and monoclonal mouse 2H11 antibody against bovine profilin was described elsewhere (Mayboroda *et al.*, 1997). Both anti-profilin antibodies selectively interact with profilin I and not with profilin II. Rabbit polyclonal 119 anti-RhoA antibody and mouse monoclonal 26C4 anti-RhoA antibody (Lang *et al.*, 1993) were obtained from Santa Cruz Biotechnology, Inc. Mouse monoclonal 9E10 anti-myc antibody (Evan *et al.*, 1985) was a gift of S.Nishikawa, Kyoto University.

These antibodies were depleted by incubating an aliquot of AP50, 2H11 and 119 solution successively with five pieces of membranes blotted with GST–cl.50, purified profilin and GST–RhoA, respectively. The antibody-depleted solution was used at the same dilution as the original antibody.

Affinity precipitation of p140mDia by Rho family proteins in vitro

GST fusion proteins of RhoA, Rac1 and Cdc42Hs were expressed and prepared according to the manufacturer's protocol. Confluent Swiss 3T3 cells, ~1×10^7 cells, were collected and disrupted by sonication (5 s, four times) in 3.2 ml of buffer A [10 mM MES pH 6.5, 150 mM NaCl, 2 mM $MgCl_2$, 0.5 mM EDTA, 0.5% Triton X-100, 5 mM dithiothreitol (DTT), 1 mM phenylmethylsulfonyl fluoride (PMSF), 5 μg/ml leupeptin]. Sonicated homogenates were centrifuged at 10 000 *g* for 20 min, and the supernatant was saved. Loading of each nucleotide was carried out by incubating 10 μM GST–Rho GTPases with 1 mM GTPγS or GDP under the same conditions as described previously (Ishizaki *et al.*, 1996). One-tenth of the supernatant was then incubated with 400 pmol of each nucleotide-loaded GST–Rho GTPase. After incubation at 30°C for 30 min, 5 μl of glutathione–Sepharose4B was added to the solution and the mixture was incubated at 4°C for 1 h. The beads were washed twice with 1 ml of buffer A, and boiled in Laemmli sample buffer. The solubilized extracts were subjected to immunoblotting with anti-cl.50 antiserum according to the procedure previously published (Kumagai *et al.*, 1993).

Cells and immunofluorescence

Swiss 3T3 cells, sMDCK2 cells stably expressing myc-tagged RhoA (Takaishi *et al.*, 1995) (a gift of K.Takaishi and Y.Takai) and HT1080 human fibrosarcoma cells (a gift of K.Sekiguchi) were grown in Dulbecco's modified Eagle's medium (DMEM) supplemented with 10% fetal calf serum (FCS). sMDCK2 cells were maintained in 500 μg/ml G-418. For morphological analysis, HT1080 and Swiss 3T3 cells were seeded onto glass coverslips at a density of 1×10^5 cells per 35 mm dish, cultured overnight and fixed. sMDCK2 cells were seeded onto glass coverslips at a density of 1×10^4 cells per 35 mm culture dish in DMEM containing 10% FCS, and incubated for 16 h. The medium was then changed to DMEM without FCS, and the cells were incubated for another 24 h. Serum-starved cells were stimulated with or without 10^{-7} M TPA (Sigma) for 15 min at 37°C, and fixed.

For indirect immunofluorescence, cells were fixed in phosphate-buffered saline (PBS) containing 3.7% paraformaldehyde for 20 min at room temperature, and then permeabilized with 0.2% Triton X-100 in PBS for 10 min. After several washes with PBS, cells were incubated in buffer B (20 mM Tris pH 7.4, 50 mM NaCl) containing 5% BSA at room temperature for >30 min. For staining with rabbit polyclonal antibodies, the cells were incubated either with a 1:10 dilution of AP50 for p140mDia staining, with a 1:40 polyclonal anti-RhoA antibody, or with a 1:80 dilution of anti-profilin antiserum in the blocking solution at room temperature for 1 h, and washed three times with buffer B containing 0.1% Triton X-100. The cells were then stained with Cy2-labeled goat anti-rabbit IgG (Amersham Life Science) and washed five times with buffer B plus 0.1% Triton X-100. For dual immunofluorescence, either 9E10 anti-Myc antibody at 10 μg/ml, 2H11 monoclonal anti-profilin antibody at a 1:2 dilution or 26C4 monoclonal anti-RhoA antibody at a 1:50 dilution, was added to the primary antibody incubation. Rhodamine-conjugated anti-mouse IgG (Organon Technica Corp.) was then used at a 1:50 dilution. For F-actin staining, rhodamine-conjugated phalloidin (Molecular Probe) was added to the second antibody incubation. Nuclear staining with DAPI (4′,6-diamidino-2-phenylindole) was performed as described (Dyck *et al.*, 1994). Fluorescence images were photographed with a conventional fluorescence microscope (Axiophoto, Zeiss) or with a confocal laser scanning microscope (MRC1024, Bio-Rad).

In some experiments, COS cells overexpressing p140mDia were first washed with a buffer containing 10 mM MES, pH 6.1, 150 mM NaCl, 5 mM EGTA, 5 mM $MgCl_2$ and 5 mM glucose, and extracted with 0.1% Triton X-100 in this buffer in the presence of 10 μM phalloidin for 10, 30 and 300 s before fixation.

Latex bead binding and microinjection in Swiss 3T3 cells

Polystyrene latex beads (11.9 μm average diameter, Sigma) were coated with either 50 μg/ml human FN (Collaborative Research, Inc.) or

100 μg/ml poly-L-lysine (PLL) (Sigma) as described (Grinnel and Geiger, 1986). Trypsinized Swiss 3T3 cells were plated onto FN-coated coverslips and allowed to attach to the slips for 2 h at 37°C in DMEM containing 10% FCS. Each different type of beads was then placed onto the cells. After incubation for 15 min at 37°C, the cells were fixed. For microinjection of C3 exoenzyme, recombinant C3 exoenzyme was prepared as described (Morii and Narumiya, 1995). C3 exoenzyme at 150 ng/μl in 10 mM HEPES pH 7.2, 2 mM $MgCl_2$, 20 mM KCl and 0.1 mM DTT was injected into the cells, plated and attached as described, with 0.5 μg/μl rabbit IgG or mouse IgG (Zymed) for the detection of injected cells. After the cells were incubated for 20–30 min, binding of FN-coated beads was then carried out as described above.

Profilin–agarose-binding assay

Human platelet profilin was purified using PLP affinity chromatography, as described previously (Janmey, 1991). Briefly, 250 mg of PLP (M_r 12 000, Sigma) was coupled to CNBr-activated Sepharose 4B (Pharmacia). Washed human platelets were prepared from the buffy coat fraction of 100 U of blood as described (Ishizaki *et al.*, 1996). The platelets were disrupted in 200 ml of extraction buffer, and the supernatants were applied to the PLP–Sepharose. The homogenous preparation of profilin was obtained by the elution with 7 M urea after 4 M urea washes. Profilin, 0.96 mg, was then conjugated with 1 ml of NHS-HiTrap (Pharmacia) according to the manufacturer's protocol (immobilized profilin). As a control, the same amount of BSA was similarly coupled to NHS-HiTrap. Rho family GTPases were prepared as GST fusion proteins as described, cleaved from GST according to the manufacturer's protocol, and loaded with GTPγS or GDP as described above. Confluent Swiss 3T3 cells obtained from twelve 6 cm dishes were solubilized in 2.4 ml of buffer C (10 mM Tris–HCl, pH 7.0, 150 mM NaCl, 50 mM NaF, 2 mM $MgCl_2$, 0.5 mM EDTA, 1 mM Na_3VO_4, 0.1% Triton X-100, 1 mM PMSF, 1 mM benzamidine, 5 μg/ml leupeptin) and centrifuged at 10 000 *g* for 10 min. A one-tenth aliquot of the supernatant was then incubated with 20 μl of immobilized profilin with the addition of free GTPγS or GDP, a GTPγS- or GDP-loaded Rho family GTPase, or a vehicle. The final concentration of Rho GTPases added was 1 μM. After the mixture was incubated for 30 min at 25°C, the beads were spun down at 1000 *g* for 2 min. The supernatant was saved. The beads were washed once with 100 μl of buffer C containing 300 mM NaCl. Half of the washed beads and one-tenth of the saved supernatant were boiled in Laemmli buffer and subjected to anti-p140mDia immunoblotting using the ECL system (Amersham).

Construction of the expression vector for p140mDia and transfection

pCMX-p140mDia was constructed by sequentially ligating in pCMX vector (Dyck *et al.*, 1994) the *Eco*RI–*Bam*HI fragment of clone 504 cDNA subcloned in pBluescript, the *Bam*HI–*Eco*RI fragment of clone 503 cDNA in pBluescript and the *Eco*RI–*Eco*RI fragment of clone E51 cDNA in pBluescript. Construction of a mammalian expression vector of C3 exoenzyme, pEFBOS-C3, will be described elsewhere. Transfection of COS-7 cells with either pCMX-p140mDia, pEFBOS-C3, pCMX-FLAG-Val14-RhoA, or in combination, was performed as described (Ishizaki *et al.*, 1996; Watanabe *et al.*, 1996). The cells were fixed 25 h after the addition of plasmid DNA, and stained with anti-p140mDia, anti-FLAG M2 antibody (Kodak) or rhodamine–phalloidin as described above.

Acknowledgements

We are indebted to Stan Hollenberg, Rolf Sternglanz, Stan Fields and Paul Bartel for the yeast two-hybrid system and to Kenji Takaishi and Yoshimi Takai for sMDCK2 cells, pGEX-Rac1 and pGEX-Cdc42Hs. We thank S.Nishikawa for 9E10 antibody, K.Sekiguchi for HT1080 cells and M.Symons for discussion. We are most grateful to Y.Kishimoto and H.Fuyuhiro for their skilled assistance and to K.Okuyama for secretarial work. We also thank T.Murata and H.Boku for help in the preparation of antibody, O.Nakagawa for a mouse cDNA library and K.Fujisawa for pEFBOS-C3. This work was supported in part by a Grant-in-Aid for Specially Promoted Research from the Ministry of Education, Science and Culture of Japan and by a HFSP grant.

References

Adam,T., Giry,M., Boquet,P. and Sansonetti,P. (1996) Rho-dependent membrane folding causes *Shigella* entry into epithelial cells. *EMBO J.*, **15**, 3315–3321.

Adamson,P., Paterson,H.F. and Hall,A. (1992) Intracellular localization of the $p21^{rho}$ proteins. *J. Cell Biol.*, **119**, 617–627.

Aullo,P., Giry,M., Olsnes,S., Popoff,M.R., Kocks,C. and Boquet,P. (1993) A chimeric toxin to study the role of the 21 kDa GTP binding protein rho in the control of actin microfilament assembly. *EMBO J.*, **12**, 921–931.

Balasubramanian,M.K., Hirani,B.R., Burke,J.D. and Gould,K.L. (1994) The *Schizosaccharomyces pombe* $cdc3^+$ gene encodes a profilin essential for cytokinesis. *J. Cell Biol.*, **125**, 1289–1301.

Burbelo,P.D., Drechsel,D. and Hall,A. (1995a) A conserved binding motif defines numerous candidate target proteins for both Cdc42 and Rac GTPases. *J. Biol. Chem.*, **270**, 29071–29074.

Burbelo,P.D., Miyamoto,S., Utani,A., Brill,S., Yamada,K.M., Hall,A. and Yamada,Y. (1995b) p190-B, a new member of the Rho GAP family, and Rho are induced to cluster after integrin cross-linking. *J. Biol. Chem.*, **270**, 30919–30926.

Buß,F., Temm-Grove,C., Henning,A. and Jockusch,B.M. (1992) Distribution of profilin in fibroblasts correlates with the presence of highly dynamic actin filaments. *Cell Motil. Cytoskel.*, **22**, 51–61.

Cao,L.-G., Babcock,G.G., Rubenstein,P.A. and Wang,Y.-L. (1992) Effects of profilin and profilactin on actin structure and function of living cells. *J. Cell Biol.*, **117**, 1023–1029.

Castrillon,D.H. and Wasserman,S.A. (1994) diaphanous is required for cytokinesis in *Drosophila* and shares domains of similarity with the products of the limb deformity gene. *Development*, **120**, 3367–3377.

Chong,L.D., Traynor-Kaplan,A., Bokoch,G.M. and Schwartz,M.A. (1994) The small GTP-binding protein Rho regulates a phosphatidylinositol 4-phosphate 5-kinase in mammalian cells. *Cell*, **79**, 507–513.

Dyck,J.A., Maul,G.G., Miller,W.H.,Jr, Chen,J.D., Kakizuka,A. and Evans,R.M. (1994) A novel macromolecular structure is a target of the promyelocyte-retinoic acid receptor oncoprotein. *Cell*, **76**, 333–343.

Emmons,S., Phan,H., Calley,J., Chen,W., James,B. and Manseau,L. (1995) *cappuccino*, a *Drosophila* maternal effect gene required for polarity of the egg and embryo, is related to the vertebrate *limb deformity* locus. *Genes Dev.*, **9**, 2482–2494.

Evan,G.I., Lewis,G.K., Ramsay,G. and Bishop,J.M. (1985) Isolation of monoclonal antibodies specific for human c-*myc* proto-oncogene product. *Mol. Cell. Biol.*, **5**, 3610–3616.

Goldschmidt-Clermont,P.J., Machesky,L.M., Doberstein,S.K. and Pollard,T.D. (1991) Mechanism of the interaction of human platelet profilin with actin. *J. Cell Biol.*, **113**, 1081–1089.

Grinnell,F. and Geiger,B. (1986) Interaction of fibronectin-coated beads with attached and spread fibroblasts; binding, phagocytosis and cytoskeletal reorganization. *Exp. Cell Res.*, **162**, 449–461.

Hart,M.J., Eva,A., Zangrilli,D., Aaronson,S.A., Evans,T., Cerione,R.A. and Zheng,Y. (1994) Cellular transformation and guanine nucleotide exchange activity are catalyzed by a common domain on the *dbl* onocogene product. *J. Biol. Chem.*, **269**, 62–65.

Hartwig,J.H., Bokoch,G.M., Carpenter,C.L., Janmey,P.A., Taylor,L.A., Toker,A. and Stossel,T.P. (1995) Thrombin receptor ligation and activated Rac uncap actin filament barbed ends through phosphoinositide synthesis in permeabilized human platelets. *Cell*, **82**, 643–653.

Hartwig,J.H., Chambers,K.A., Hopcia,K.L. and Kwiatkowski,D.J. (1989) Association of profilin with filament-free regions of human leukocyte and platelet membranes and reversible membrane binding during platelet activation. *J. Cell. Biol.*, **109**, 1571–1579.

Haugwitz,M., Noegel,A.A., Karakesisoglou,J. and Schleicher,M. (1994) *Dictyostelium amoebae* that lack G-actin-sequestering profilins show defects in F-actin content, cytokinesis and development. *Cell*, **79**, 303–314.

Ishizaki,T. *et al.* (1996) The small GTP-binding protein Rho binds to and activates a 160 kDa Ser/Thr protein kinase homologous to myotonic dystrophy kinase. *EMBO J.*, **15**, 1885–1893.

Jackson-Grusby,L., Kuo,A. and Leder,P. (1992) A variant limb deformity transcript expressed in the embryonic mouse limb defines a novel formin. *Genes Dev.*, **6**, 29–37.

Janmey,P.A. (1991) Polyproline affinity method for purification of platelet profilin and modification with pyrene-maleimide. *Methods Enzymol.*, **196**, 92–99.

Janmey,P.A. (1994) Phosphoinositides and calcium as regulators of cellular actin assembly and disassembly. *Annu. Rev. Physiol.*, **56**, 169–191.

Jockusch,B.M. *et al.* (1995) The molecular architecture of focal adhesions. *Annu. Rev. Cell Dev. Biol.*, **11**, 379–416.

Kimura,K. *et al*. (1996) Regulation of myosin phosphatase by Rho and Rho-associated kinase (Rho-kinase). *Science*, **273**, 245–248.

Kishi,K., Sasaki,T., Kuroda,S., Itoh,T. and Takai,Y. (1993) Regulation of cytoplasmic division of *Xenopus* embryo by rho p21 and its inhibitory GDP/GTP exchange protein (rho GDI). *J. Cell Biol.*, **120**, 1187–1195.

Kumagai,N., Morii,N., Fujisawa,K., Nemoto,Y. and Narumiya,S. (1993) ADP-ribosylation of rho p21 inhibits lysophosphatidic acid-induced protein tyrosine phosphorylation and phosphatidylinositol 3-kinase activation in cultured Swiss 3T3 cells. *J. Biol. Chem.*, **268**, 24535–24538.

Kunkel,T.A. (1985) Rapid and efficient site-specific mutagenesis without phenotypic selection. *Proc. Natl Acad. Sci. USA*, **82**, 488–492.

Lang,P., Gesbert,F., Thiberge,J.-M., Troalen,F., Dutartre,H., Chavrier,P. and Bertoglio,J. (1993) Characterization of a monoclonal antibody specific for the Ras-related GTP-binding protein RhoA. *Biochem. Biophys. Res. Commun.*, **196**, 1522–1528.

Leung,T., Manser,E., Tan,L. and Lim,L. (1995) A novel serine/threonine kinase binding the Ras-related RhoA GTPase which translocates the kinase to peripheral membranes. *J. Biol. Chem.*, **270**, 29051–29054.

Mabuchi,I., Hamaguchi,Y., Fujimoto,H., Morii,N., Mishima,M. and Narumiya,S. (1993) A rho-like protein is involved in the organisation of the contractile ring in dividing sand dollar eggs. *Zygote*, **1**, 325–331.

Machesky,L.M. and Pollard,T.D. (1993) Profilin as a potential mediator of membrane–cytoskeleton communication. *Trends Cell Biol.*, **3**, 381–385.

Madaule,P., Furuyashiki,T., Reid,T., Ishizaki,T., Watanabe,G., Morii,N. and Narumiya,S. (1995) A novel partner for the GTP-bound forms of rho and rac. *FEBS Lett.*, **377**, 243–248.

Marhoul,J.F. and Adams,T.H. (1995) Identification of developmental regulatory genes in *Aspergillus nidulans* by overexpression. *Genetics*, **139**, 537–547.

Matsui,T. *et al*. (1996) Rho-associated kinase, a novel serine/threonine kinase, as a putative target for the small GTP binding protein Rho. *EMBO J.*, **15**, 2208–2216.

Mayboroda,O., Schluter,K. and Jockusch,B.M. (1997) Differential association of profilin with microfilaments in PtK2 cells. *Cell Motil. Cytoskel.*, in press.

Miyamoto,S., Teramoto,H., Coso,O.A., Gutkind,J.S., Burbelo,P.D., Akiyama,S.K. and Yamada,K.M. (1995) Integrin function: molecular hierarchies of cytoskeletal and signaling molecules. *J. Cell Biol.*, **131**, 791–805.

Mockrin,S.C. and Korn,E.D. (1980) *Acanthamoeba* profilin interacts with G-actin to increase the rate of exchange of actin-bound adenosine 5′-triphosphate. *Biochemistry*, **19**, 5359–5362.

Morii,N. and Narumiya,S. (1995) Preparation of native and recombinant *Clostridium botulinum* C3 ADP-ribosyltransferase and identification of Rho proteins by ADP-ribosylation. *Methods Enzymol.*, **256**, 196–206.

Morii,N., Teru-uchi,T., Tominaga,T., Kumagai,N., Kozaki,S., Ushikubi,F. and Narumiya,S. (1992) A rho gene product in human blood platelets. II. Effects of the ADP-ribosylation by botulinum C3 ADP-ribosyltransferase on platelet aggregation. *J. Biol. Chem.*, **267**, 20921–20926.

Nakagawa,O., Fujisawa,K., Ishizaki,T., Saito,Y., Nakao,K. and Narumiya,S. (1996) ROCK-I and ROCK-II, two isoforms of Rho-associated coiled-coil forming protein serine/threonine kinase in mice. *FEBS Lett.*, **392**, 189–193.

Nishida,E. (1985) Opposite effects of cofilin and profilin from porcine brain on rate of exchange of actin-bound adenosine 5′-triphosphate. *Biochemistry*, **24**, 1160–1164.

Nishiyama,T., Sasaki,T., Takaishi,K., Kato,M., Yaku,H., Araki,K., Matsuura,Y. and Takai,Y. (1994) rac p21 is involved in insulin-induced membrane ruffling and rho p21 is involved in hepatocyte growth factor- and 12-O-tetradecanoylphorbol-13-acetate (TPA)-induced membrane ruffling in KB cells. *Mol. Cell. Biol.*, **14**, 2447–2456.

Nobes,C.D. and Hall,A. (1995) Rho, Rac, and Cdc42 GTPases regulate the assembly of multimolecular focal complexes associated with actin stress fibers, lamellipodia, and filopodia. *Cell*, **81**, 53–62.

Pantaloni,D. and Carlier,M-F. (1993) How profilin promotes actin filament assembly in the presence of thymosin β4. *Cell*, **75**, 1007–1014.

Petersen,J., Weilguny,D., Egel,R. and Nielsen,O. (1995) Characterization of *fus1* in *Schizosaccharomyces pombe*; a developmentally controlled function needed for conjugation. *Mol. Cell. Biol.*, **15**, 3697–3707.

Rankin,S., Morii,N., Narumiya,S. and Rozengurt,E. (1994) Botulinum C3 exoenzyme blocks the tyrosine phosphorylation of p125FAK and paxillin induced by bombesin and endothelin. *FEBS Lett.*, **354**, 315–319.

Reid,T., Furuyashiki,T., Ishizaki,T., Watanabe,G., Watanabe,N., Fujisawa,K., Morii,N., Madaule,P. and Narumiya,S. (1996) Rhotekin, a new putative target for Rho bearing homology to a serine/threonine kinase, PKN, and rhophilin in the Rho-binding domain. *J. Biol. Chem.*, **271**, 13556–13560.

Reinhard,M., Giehl,K., Abel,K., Haffner,C., Jarchau,T., Hoppe,V., Jockusch,B.M. and Walter,U. (1995) The proline-rich focal adhesion and microfilament protein VASP is a ligand for profilins. *EMBO J.*, **14**, 1583–1589.

Ridley,A.J. and Hall,A. (1992) The small GTP-binding protein rho regulates the assembly of focal adhesions and actin stress fibers in response to growth factors. *Cell*, **70**, 389–399.

Rothkegel,M., Mayboroda,O., Rohde,M., Wucherpfennig,C., Valenta,R. and Jockusch,B.M. (1996) Plant and animal profilins are functionally equivalent and stabilize microfilaments in living animal cells. *J. Cell Sci.*, **109**, 83–90.

Sambrook,J., Fritsch,E.F. and Maniatis,T. (1989) *Molecular Cloning: A Laboratory Manual*. Cold Spring Harbor Laboratory Press, Cold Spring Harbor, NY.

Schutt,C.E., Myslik,J.C., Rozycki,M.D., Goonesekere,N.C.W. and Lindberg,U. (1993) The structure of crystalline profilin–β-actin. *Nature*, **365**, 810–816.

Seckl,M.J., Morii,N., Narumiya,S. and Rozengurt,E. (1995) Guanosine 5′-3-*O*-(thio) triphosphate stimulates tyrosine phosphorylation of $p125^{FAK}$ and paxillin in permeabilized Swiss 3T3 cells. *J. Biol. Chem.*, **270**, 6984–6990.

Stephen,A.F., Gish,W., Miller,W., Myers,E.W. and Lipman,D. (1990) Basic local search tool. *J. Mol. Biol.*, **215**, 403–410.

Symons,M., Derry,J.M.J., Karlak,B., Jiang,S., Lemahieu,V., McCormick,F., Francke,U. and Abo,A. (1996) Wiskott–Aldrich syndrome protein, a novel effector for the GTPase CDC42Hs, is implicated in actin polymerization. *Cell*, **84**, 723–734.

Takaishi,K., Kikuchi,A., Kuroda,S., Kotani,K., Sasaki,T. and Takai,Y. (1993) Involvement of rho p21 and its inhibitory GDP/GTP exchange protein (rho GDI) in cell motility. *Mol. Cell. Biol.*, **13**, 72–79.

Takaishi,K., Sasaki,T., Kameyama,T., Tsukita,S., Tsukita,S. and Takai,Y. (1995) Translocation of activated Rho from the cytoplasm to membrane ruffling area, cell–cell adhesion sites and cleavage furrows. *Oncogene*, **11**, 39–48.

Tanaka,M. and Shibata,H. (1985) Poly(L-proline)-binding proteins from chick embryos are a profilin and a profilactin. *Eur. J. Biochem.*, **151**, 291–297.

Theriot,J.A., Rosenblatt,J., Portnoy,D.A., Goldschmidt-Clermont,P.J. and Mitchison,T.J. (1994) Involvement of profilin in the actin-based motility of *L.monocytogenes* in cells and in cell-free extracts. *Cell*, **76**, 505–517.

Tominaga,T., Sugie,K., Hirata,M., Morii,N., Fukata,J., Uchida,A., Imura,H. and Narumiya,S. (1993) Inhibition of PMA-induced, LFA-1-dependent lymphocyte aggregation by ADP-ribosylation of the small molecular weight GTP-binding protein, rho. *J. Cell Biol.*, **120**, 1529–1537.

Verheyen,E.M. and Cooley,L. (1994) Profilin mutations disrupt multiple actin-dependent processes during *Drosophila* development. *Development*, **120**, 717–728.

Vojtek,A.B., Hollenberg,S.M. and Cooper,J.A. (1993) Mammalian Ras interacts directly with the serine/threonine kinase Raf. *Cell*, **74**, 205–214.

Watanabe,G. *et al*. (1996) Protein kinase-N (PKN) and PKN-related protein rhophilin as targets of small GTPase Rho. *Science*, **271**, 645–648.

Woychik,R.P., Maas,R.L., Zeller,R., Vogt,T.F. and Leder,P. (1990) 'Formins': proteins deduced from the alternative transcripts of the limb deformity gene. *Nature*, **346**, 850–853.

Received on October 31, 1996; revised on February 26, 1997

Note added in proof

Bni1p was recently reported to be a putative target of Rho1p or Cdc42p of *Saccharomyces cerevisiae* [Kohno *et al*. (1996) *EMBO J.*, **15**, 6060–6068; Evangelista *et al*. (1997) *Science*, **276**, 118–122]. The ROCK/ROKα/Rho-kinase family of protein kinases have been shown to mediate Rho-induced formation of focal adhesions and stress fibers [Leung *et al*. (1996) *Mol. Cell. Biol.*, **16**, 5313–5327; Amano *et al*. (1997) *Science*, **275**, 1308–1311; Ishizaki *et al*. (1997) *FEBS Lett.*, **404**, 118–124].